Journal of Applied Pharmaceutical Research
Volume 12 Issue 4, Year of Publication 2024, Page 124 – 138
DOI: https://doi.org/10.69857/joapr.v12i4.590

Check for updates

Research Article

JOURNAL OF APPLIED PHARMACEUTICAL RESEARCH | JOAPR
www.japtronline.com ***ISSN: 2348 – 0335***

OPTIMIZATION AND EVALUATION OF NEBIVOLOL HYDROCHLORIDE LOADED TRANSFEROSOMES USING BOX-BEHNKEN EXPERIMENTAL DESIGN

P V Shelke[1]*, Punit R Rachh[1], Someshwar Mankar[2], Saurin Amin[3], Deepak Jain[4]

Article Information
Received: 8th April 2024
Revised: 14th June 2024
Accepted: 8th July 2024
Published: 31st August 2024

Keywords
Transferosomes, Hypertension, Nebivolol hydrochloride, Box-Behnken design, Stability study

ABSTRACT
Background: This study optimizes and evaluates transferosomes containing Nebivolol Hydrochloride to enhance the drug's bioavailability and therapeutic efficacy. Ultra-deformable vesicles called transferosomes help to increase drug administration via the skin. **Methodology**: Using a thin-film hydration technique, beta-blocker Nebivolol Hydrochloride, which has antihypertensive properties, was added to transferosomes. To attain the ideal vesicle size (between 200 to 300 nm), entrapment efficiency, and deformability, the formulation was adjusted by adjusting the amounts of phosphatidylcholine, Span 80, and hydration time using a Box-Behnken experimental design. Particle size analysis, zeta potential measurement, and in vitro drug release tests were performed to characterize the transferosomes. **Results and discussion**: The optimized formulation demonstrated notable deformability, an entrapment effectiveness of 50%, and a vesicle size of 265 nm. The Box-Behnken design made it easier to evaluate the interactions between variables systematically. In vitro drug release studies showed a drug diffusion that persisted for a whole day, suggesting that transferosomes may have long-lasting therapeutic effects. Stability studies at room temperature and accelerated conditions over six months confirmed the formulation's robustness. **Conclusion**: The results imply that Nebivolol Hydrochloride transferosome-based delivery may be a viable strategy for improving the drug's bioavailability and effectiveness, as nearly 100% of drugs diffuse within 24 hr, perhaps leading to a breakthrough in the management of hypertension.

INTRODUCTION

One approach to administering drugs that has shown promise for both local and systemic delivery is transdermal administration. Compared to oral dosage forms, it has several benefits, such as increased patient adherence during long-term therapy [1], first-pass metabolism bypassed [2], sustained drug release, maintenance of constant plasma drug levels [3], decreased patient variability [4], and the option to stop treatment when

[1]*Department of Pharmaceutical Science, Bhagwant University, Ajmer, Rajasthan, India*
[2]*Pravara Rural College of Pharmacy, Loni, Maharashtra, India*
[3]*Gujarat Technological University, Gujarat, India*
[4]*Senores Pharmaceuticals Pvt. Ltd., One42 South Tower, Ashok Vatika, Ahmedabad, Gujarat 380058 India*

For Correspondence: **pravinshelke04@gmail.com**

needed. Transdermal administration is also a better choice for those with delicate digestive systems since it helps lessen the gastrointestinal side effects of oral drugs [5]. However, the structural barrier of the stratum corneum prevents medications from penetrating. Thus, it must be modified to make it easier to administer pharmaceuticals that penetrate poorly [6]. As a selective β1-adreno receptor blocker, Nebivolol hydrochloride exhibits distinct hemodynamic properties, including a reduction in peripheral vascular resistance and a neutral effect on cardiac output. Clinical research has validated its effectiveness and safety in lowering blood pressure by vasodilation. Nebivolol hydrochloride has favorable properties such as low molecular weight, short half-life, moderate lipophilicity, and low dosage requirement, which make it an excellent choice for transdermal drug delivery, even if its limited oral bioavailability (varying between 12% to 96%) is caused by extensive metabolism [7]. Nebivolol hydrochloride counteracts the effects of epinephrine by specifically inhibiting β1-receptors, hence reducing blood pressure and heart rate [8]. Furthermore, β blockers prevent the production of renin, which narrows blood vessels. Nebivolol hydrochloride may also bind β2-receptors at higher doses [9].

Pharmaceutical research has shifted its primary attention to developing sophisticated drug delivery systems to improve the effectiveness and bioavailability of medicinal medicines. Ultra-deformable lipid vesicles known as transferosomes are a significant advancement in this field that show promise for the transdermal delivery of various medications. Transferosomes are designed to be more deformable than traditional liposomes or other vesicular systems. Their ability to squeeze through the skin's pores allows for better penetration into the dermal layers, improving the bioavailability of the drug [10]. The main focus of this work is the optimization and assessment of transferosomes containing the beta-blocker nebivolol hydrochloride, which is frequently used to treat hypertension. The goal of encasing Nebivolol Hydrochloride in transferosomes is to enhance its transdermal permeability and therapeutic efficacy, which may lead to a decrease in dosage frequency and a reduction in systemic side effects.

A response surface methodology called Box-Behnken experimental design methodically investigates the interplay of several formulation variables [11]. This design evaluates the impact of these variables on important quality attributes such as vesicle size, entrapment efficiency, and drug release profile, which helps with the precise optimization of the transferosomal formulation. This study's combination of these cutting-edge analytical and experimental methodologies highlights an accurate and thorough approach. The ultimate goal of the results of this research is to improve patient outcomes in the treatment of hypertension by providing essential insights into the composition of transferosomes for increased transdermal distribution of Nebivolol hydrochloride.

MATERIALS AND METHODS

Materials

Sun Pharmaceutical Industries Ltd, Baroda, generously provided nebivolol hydrochloride. Phosphatidylcholine, Span 80, was procured from Sigma Aldrich, India. All additional solvents, including methanol and chloroform, were analytical grade. Double-distilled water was prepared in the laboratory for the study. All materials met USP 24 standards and were purchased from ACS Chemical Pvt. Ltd., Ahmedabad, India.

Preparation of Transferosomes

Transferosomes have been made utilizing the usual rotary evaporation-sonication technique [12,13]. Phosphatidylcholine was precisely combined with an edge activator, Span 80, in a sterile and dry round bottom flask. The lipid mixture was dissolved in an organic solvent mixture (Methanol: Chloroform, 1:1). The organic solvent was eliminated using a rotary evaporator higher than the lipid transition temperature. Any residual residues of the solvent were eradicated by subjecting them to vacuum conditions overnight. The lipid film was hydrated with phosphate-buffered saline (PBS) at a pH of 7.4, which included Nebivolol Hydrochloride (NBH) to get the required drug concentration. The combination underwent rotational agitation for 1 hour at a designated temperature. The resultant vesicles were subsequently permitted to expand for 2 hours at ambient temperature to generate transferosomes. The dense mixture obtained was subjected to ultrasonic treatment for 30 minutes at a temperature of 4°C and a frequency of 50 kHz to reach the targeted vesicle size of 100-300 nm [14].

Box-Behnken Design for transferosomes

A systematic approach using the Box-Behnken design was used to optimize formulation-independent elements such as critical material attributes (CMA), the amount of phosphatidylcholine (mg), the concentration of Span 80 (%), and necessary process parameter (CPP), the hydration time (min). This statistical

technique is beneficial for determining the ideal conditions and comprehending how various factors interact [15]. The purpose of the study was to assess the relationship between these independent variables and the dependent variables, namely vesicle size (nm), polydispersity index (PDI), Zeta potential (mV), and entrapment efficiency (%), which are essential to transferosome function. Each element was investigated at three different levels in this study. Based on early research, the phosphatidylcholine, Span 80, and hydration time amounts were carefully selected to encompass a range of possible ideal values. As shown in Table 1, 13 experimental batches were created using Design-Expert software (DoE), and the significance level was chosen at $p < 0.05$. This approach offers a thorough comprehension of the formulation process by enabling the assessment of individual effects and insights into the interaction effects between the elements.

Table 1: Box-Behnken experimental design for NBH transferosomes

Formulation	Independent variables		
	X_1[a]	X_2[b]	X_3[c]
F1	-1	-1	0
F2	1	-1	0
F3	-1	1	0
F4	1	1	0
F5	-1	0	-1
F6	1	0	-1
F7	-1	0	1
F8	1	0	1
F9	0	-1	-1
F10	0	1	-1
F11	0	-1	1
F12	0	1	1
F13	0	0	0
Factor	Level		
	-1	0	1
X_1 (Amount of phosphatidylcholine, mg)	200	250	300
X_2 (Concentration of Span 80, %)	0.5	0.75	1
X_3 (Hydration time, min)	30	60	90

Physical evaluation of NBH transferosomes

The transferosomes were assessed for their particle size, polydispersity index (PDI), and zeta potential using a dynamic light scattering device (Malvern Zetasizer Ultra). For the analysis, 1 ml from every batch was added to a transparent cuvette designed to measure zeta potential and placed in the equipment. This technique offers comprehensive measurements of the particle size distribution, ensuring a precise evaluation of the PDI and the surface charge (zeta potential) of the transferosomes. These parameters are crucial for assessing the stability and homogeneity of the formulations [16,17].

Entrapment efficiency

The overall drug entrapment in all formulations was evaluated by extracting a 1 ml sample and diluting it using methanol till a homogeneous and precise mixture was achieved. The resulting mixture was subsequently examined using the UV technique. To quantify the quantity of unbound drug, an additional 1 ml of the formulation was added to a centrifugal filter tube and then centrifuged for 30 minutes. The collected filtrate containing the unbound medication was diluted with methanol, and its concentration was quantified using UV spectrophotometry (at a wavelength of 282.5 nm). The entrapment efficiency (%EE) was determined by applying equation 1 [18].

$$\%EE = \frac{Total\ drug\ conc. - Unentrapped\ drug\ conc.}{Total\ drug\ conc.} \times 100$$

In Vitro Drug Diffusion Study

In vitro drug diffusion tests were performed using Franz diffusion cells with a diffusion area of 2 cm^2. These tests were conducted at different time intervals for optimized transferosomes. An egg membrane was placed between the donor and acceptor sections, where the transferosomes were put into the membrane [19]. The egg membrane is an appropriate model for replicating skin permeability because it has structural and functional similarities to human skin. Its two-layered nature, mainly composed of proteins and glycoproteins, resembles the epidermis' lipid bilayer, allowing for realistic interactions with medication molecules [20].

The receptor compartment contained phosphate buffer at pH 7.4, which was constantly stirred using a Teflon-covered magnetic stirrer. To simulate physiological environments, the temperature of the diffusion cell was conserved at 37±1°C. The concentration of the NBH in 1mL samples obtained at regular intervals during the 24 hours was measured using a UV-visible spectrophotometer (at a wavelength of 282.5 nm). To prepare the egg membranes, the contents of the eggs were removed, and the

shells were immersed in weak hydrochloric acid for 45 minutes. The outer membranes were then gently detached from the shells and adequately cleaned with distilled water to eliminate any remaining acid and impurities.

Stability study

For six months, the optimized transferosomes were placed in a stability chamber at 40 ± 2°C and 75 ± 5% relative humidity following ICH recommendations for accelerated stability tests [21]. USP type-1 flint vials containing this formulation were filled and covered with aluminum caps. After being removed from the samples every 3 months, the physical appearance, drug content, and zeta potential were assessed [22].

RESULTS AND DISCUSSION

In the present work, transferosomes loaded with NBH were synthesized, manufactured, and assessed for transdermal delivery appropriateness to solve the inherent difficulties in delivering NBH orally. To be more precise, we used phospholipids, which create a lipidic bilayer, and a combination of biocompatible and non-toxic surfactants - Span - to make the transferosomes [23]. This strategy was used to get around the main drawbacks of oral administration techniques.

Optimization of CMA and CPP for NBH transferosomes

An extensive investigation was carried out to determine the impact of critical material attributes and critical process parameters using a Box–Behnken experimental design methodology, which includes a three-factor, three-level approach. The investigation was performed by statistical software (Design-Expert version 13) and validated through ANOVA at a significance level of 0.05 [24]. These included the amount of phosphatidylcholine (X1), the concentration of Span 80 (X2), and the hydration time (X3). Owing to its ability to reduce trial runs more effectively than central composite designs, the Box–Behnken design was intentionally chosen. Based on data from 13 trial runs, the Design Expert software produced a design matrix; Table 2 shows the results of these formulations. The contour plots that were created for each response variable, i.e., vesicle size (Y1), polydispersity index (Y2), Zeta potential (Y3), and entrapment efficiency (Y4), helped decipher combined factor effects on response outcomes and for assessing variable-response interactions. Table 3 shows the response observed in each formulation. Additionally, a quantitative assessment was conducted by comparing the experimental response values with the predicted values, displayed using linear correlation plots.

Table 2 Results of NBH Transferosome Formulation Characterization

Batch	Vesicle size, nm (Y1)	Polydispersity index (Y2)	Zeta potential, mV (Y3)	Entrapment efficiency, % (Y4)
F1	468.36 ± 21.47	0.71 ± 0.03	-2.33 ± 0.09	57.34 ± 3.46
F2	499.61 ± 17.33	0.12 ± 0	-9.26 ± 0.27	61.75 ± 2.83
F3	146.23 ± 10.19	0.31 ± 0.01	-16.42 ± 0.45	42.34 ± 1.64
F4	547.75 ± 24.32	0.19 ± 0	-13.85 ± 0.63	64.18 ± 3.93
F5	139.62 ± 14.87	0.72 ± 0.01	-7.28 ± 0.18	40.14 ± 2.41
F6	449.21 ± 18.23	0.15 ± 0.04	-12.54 ± 0.27	54.36 ± 3.94
F7	307.55 ± 17.81	0.56 ± 0.03	-6.32 ± 0.23	45.38 ± 2.87
F8	585.37 ± 22.37	0.29 ± 0.02	-10.47 ± 0.19	65.23 ± 3.61
F9	440.78 ± 19.05	0.31 ± 0.01	-8.15 ± 0.09	51.62 ± 3.07
F10	118.64 ± 9.32	0.48 ± 0.06	-17.21 ± 0.65	39.47 ± 1.59
F11	338.57 ± 14.25	0.43 ± 0.04	-6.24 ± 0.18	57.31 ± 4.37
F12	354.32 ± 18.36	0.16 ± 0.01	-16.37 ± 0.47	53.35 ± 2.96
F13	385.35 ± 14.29	0.41 ± 0.02	-9.36 ± 0.51	50.29 ± 3.43

* All results are the mean of three observations ± SD

Applying the Box-Behnken design made it possible to conduct a systematic investigation of the response surface, which made it possible to determine the ideal parameters for the formulation procedure [24]. Regarding formulation optimization, the contour plots helped with decision-making by offering visual insights into the complex interactions between the process parameters and the answers produced. Furthermore, the regression analysis results clarify the importance of the quadratic terms in

representing the curvature of the response surfaces, supporting the comprehension of intricate interactions in the system. This thorough approach cleared the path for improved formulation development and product optimization by discovering subtle interactions in addition to the primary effects of the process factors.

Regression Analysis

All 13 batches showed a significant variation in the dependent variables (Vesicle size, PDI, ZP, and EE), which ranged from 118.64 to 585.37, 0.12 to 0.72, -17.21 to -2.33 and 39.47 to 65.23, respectively. This variation highlights how much X1, X2, and X3 impact these answers. Practical conclusions can be reached by looking at the polynomial equations and considering the magnitude and mathematical sign of the coefficients (positive or negative). Specifically, for PDI and ZP, the main effect coefficient b3 was excluded from the whole model since their p-values were more than 0.05, indicating they were insignificant. Likewise, the interaction term coefficient, b23, was removed for ZP and EE for the same reason. For all dependent variables, coefficients like b13, b11, b22, and b33 were excluded from the reduced model (RM) because their p-values were more than 0.05, indicating that they were not significant (Table 3) [24]. The logic for excluding these unimportant factors is supported by the ANOVA findings shown in Table 4. AoR, PS, and YLD high correlation coefficients signify an excellent model fit. For the vesicle size, PDI, ZP, and EE, critical F values at $\alpha = 0.05$ were found to be 9.12 (df = 4, 3), 9.01 (df = 5, 3), 8.94 (df = 6, 3) and 9.01 (df = 5, 3), in that order. Additionally, it was discovered that the computed F values (2.403 for vesicle size, 2.470 for PDI, 3.438 for ZP, and 6.359 for EE) were less than the critical levels, suggesting that there was no discernible difference between the full and reduced models (Table 4) [25].The data gathered throughout 13 batches was converted and processed with Design Expert software version 13. The analysis's findings demonstrated that vesicular size decreased when the Span 80 concentration rose since the associated coefficient, b2, was negative. Multiple linear regression analysis (see Table 3) offered additional proof of positive coefficients (b2 and b3) for size, indicating that an increase in phosphatidylcholine and hydration time would increase vesicular size. Conversely, a lower phosphatidylcholine level causes a lower PDI and ZP during EE, as shown by positive coefficients (b1) EE.

Influence of Variables on Various Response

Influence of independent variables on Vesicle Size (Y1)

After investigation, it was clear that the dependent variables significantly affected the vesicle size by selecting all dependent variables. The vesicle size varied from 118.64 nm to 585.37 nm in all formulations. Notably, F10 had the lowest vesicle size measured. After more analysis, it was discovered that the coefficient of variable X2 had a negative value (-72.55), meaning that the concentration of Span 80 had an inverse effect on the vesicle size, which means that as we increase the X2, the vesicle size increases [26].

Table 3 Regression analysis of NBH transferosomes batches

Coefficients	*Size (Y_1)*		*PDI (Y_2)*		*ZP (Y_3)*		*EE (Y_4)*	
	FM [a]	*RM* [b]	*FM*	*RM*	*FM*	*RM*	*FM*	*RM*
b_0	385.35	367.80	0.41	0.37	-9.36	-10.45	50.29	52.52
b_1	127.52	127.52	-0.19	-0.19	-1.72	-1.72	7.54	7.54
b_2	-72.55	-72.55	-0.05	-0.05	-4.73	-4.73	-3.59	-3.59
b_3[d, f]	54.70	54.70	-0.03	-	0.72	-	4.46	4.46
b_{12}	92.57	92.57	0.12	0.12	2.38	2.38	4.36	4.36
b_{23}[e, f]	84.47	84.47	-0.11	-0.11	-0.27	-	2.05	-
b_{13}[c, d, e, f]	-7.94	-	0.08	-	0.28	-	1.41	-
b_{11}[c, d, e, f]	43.75	-	0.003	-	0.87	-	3.48	-
b_{22}[c, d, e, f]	-13.61	-	-0.08	-	-1.97	-	2.64	-
b_{33}[c, d, e, f]	-58.66	-	0.02	-	-0.66	-	-2.49	-

[a] FM, Full model; [b] RM, Reduced model; [c] Nonsignificant (P>0.05) coefficients for Y_1; [d] Nonsignificant (P>0.05) coefficients for Y_2; [e] Nonsignificant (P>0.05) coefficients for Y_3; [f] Nonsignificant (P>0.05) coefficients for Y_4

Table 4 Calculation of testing the models for NBH transferosomes

Model	***df*** [c]	***SS*** [d]	***MS*** [e]	***R^2***
Vesicle size (Y_1)				
Regression				
FM[a]	9	280613.5	31179.28	0.97648
RM[b]	5	258950.7	51790.15	0.9011
Residual				Fcal = 2.403
FM	3	6759.309	2253.103	Fcritical = 9.12
RM	7	28422.07	4060.296	df = (4, 3)
Polydispersity Index (Y_2)				
Regression				
FM	9	0.479656	0.053295	0.97406
RM	4	0.42705	0.106763	0.86723
Residual				Fcal = 2.470
FM	3	0.012775	0.004258	Fcritical = 9.01
RM	8	0.065381	0.008173	df = (5, 3)
Zeta potential (Y_3)				
Regression				
FM	9	247.7416	27.52684	0.98713
RM	3	225.5312	75.17708	0.89863
Residual				Fcal = 3.438
FM	3	3.230125	1.076708	Fcritical = 8.94
RM	9	25.44048	2.82672	df = (6, 3)
Entrapment efficiency (Y_4)				
Regression				
FM	9	906.1985	100.6887	0.98832
RM	4	792.7146	198.1787	0.86455
Residual				Fcal = 6.359
FM	3	10.70695	3.568983	Fcritical = 9.01
RM	8	124.1908	15.52385	df = (5, 3)

[a] FM, Full model; [b] RM, Reduced model; [c] df, Degree of freedom; [d] SS, Sum of squares; [e] MS, Mean of squares

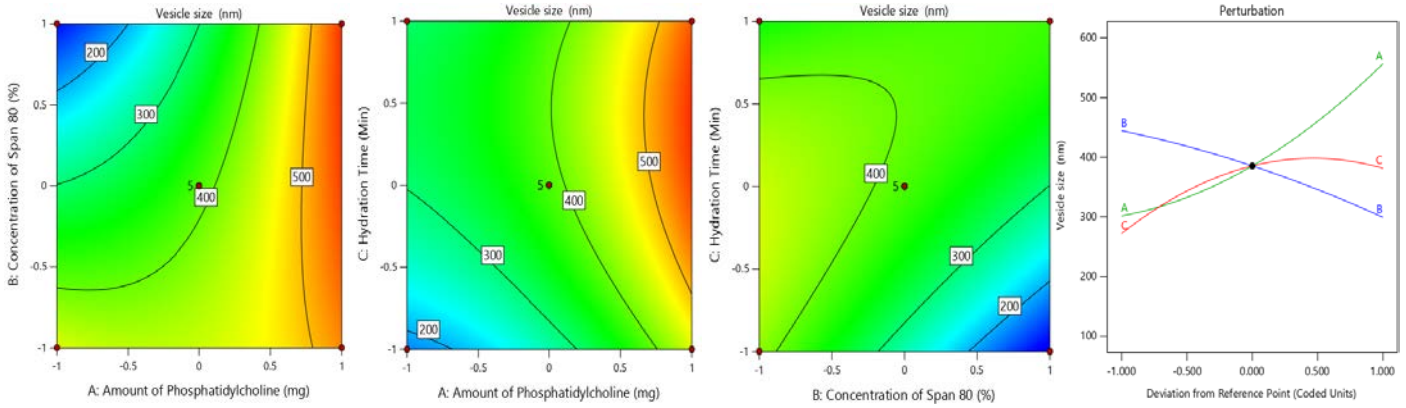

(a) (b) (c) (d)

Figure 1: Analyzing vesicle size variations with a) amount of phosphatidylcholine and concentration of Span 80, b) amount of phosphatidylcholine and hydration time, c) concentration of Span 80 and hydration time using contour plot, and d) perturbation plot.

As the amount of phosphatidylcholine increases, the X1 coefficient (127.52) on vesicle size shows a positive effect, demonstrating a direct association [27]. Figure 1's contour and perturbation plot make this link clear. The following is the polynomial equation that was obtained via regression analysis:

Vesicle Size=$385.35+127.52X_1–72.55X_2+54.70X_3+92.57X_1X_2 +84.47X_2X_3 –7.94X_1X_3 + 7.94X_1^2 – 13.61X_2^2 – 58.66X_3^2$

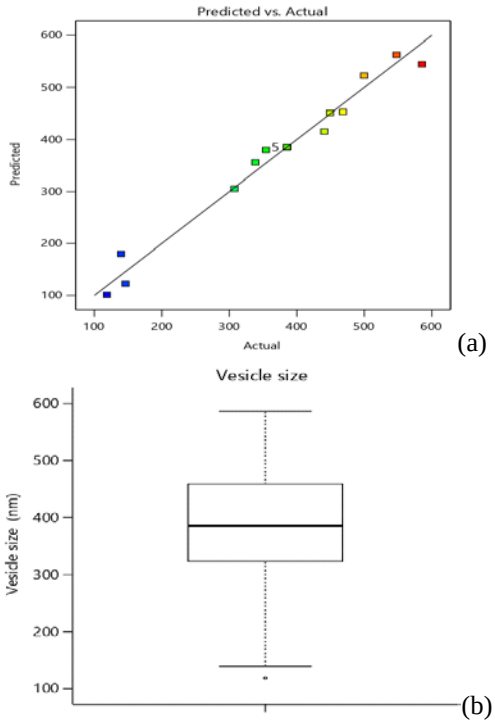

Figure 2: a) Linear correlation plot between actual and predicted values and b) Box plot for vesicle size of NBH transferosomes

Each square marker in the "Predicted vs. Actual" plot (Figure 2a) for the vesicle size of NBH transferosomes represents a pair of these data. The x-axis displays the measured vesicle sizes, while the y-axis shows the anticipated sizes. The color of the markers varies from blue in smaller sizes to red in larger sizes. A diagonal line (y = x) represents perfect agreement between forecasts and actual measurements. The line most data points closely match shows how well the model predicts the future [19]. The projected sizes closely resemble the range of actual vesicle sizes, which is about between 100 and 600 nm, indicating that the model can accurately predict vesicle sizes. The transferosome vesicle size box plot (Figure 2b) reveals that the center 50% of the sizes fall within the interquartile range (IQR), which spans from roughly 300 nm to 500 nm. The median size is approximately 400 nm. The whiskers span approximately 100 nm to 600 nm, encompassing the lowest and most significant values within 1.5 times the interquartile range. An outlier, indicating a vesicle size smaller than 100 nm, is observed beneath the lower whisker. With some variability in smaller sizes, this plot shows that most vesicle sizes are clustered between 300 and 500 nm [29,30].

Influence of independent variables on Polydispersity Index (Y2)

The analysis revealed that all the dependent factors considerably impacted the vesicle size. The range of the PDI for all formulations was 0.12 to 0.72. Additionally, the measured PDI for F2 was the lowest. Further investigation revealed that all three independent variables exhibited an inverse impact on the PDI, as indicated by the negative values of their coefficients of determination (X1, X2, and X3). The polydispersity index (PDI) is the response variable shown by the color gradient in the contour plot (Figure 3a), which shows the link between the concentration of Span 80 on the y-axis and the amount of phosphatidylcholine on the x-axis. The color bar changes from blue (lower PDI) to red (higher PDI), indicating the range of PDI values, which is 0.12 to 0.72. The blue sections represent higher phosphatidylcholine and lower Span 80 concentrations, respectively, where lower PDI values are detected, indicating more uniform particle sizes. On the other hand, lower phosphatidylcholine and higher Span 80 concentrations are associated with higher PDI values, which suggest less homogeneity [19,30]. Figure 3a helps determine the ideal formulation conditions for obtaining a low PDI by giving a visual knowledge of how changing the concentrations of phosphatidylcholine and Span 80 influences the uniformity of the transferosome sizes. Figure 3b shows the phosphatidylcholine amount on the x-axis and the hydration time on the y-axis. Plotting different polydispersity index (PDI) values reveals that the PDI tends to drop with increased phosphatidylcholine and decreasing hydration time. The PDI changes from 0.72 in the bottom left to 0.12 in the upper right. The y-axis in Figure 3c again indicates hydration time, while the x-axis shows the concentration of Span 80. The PDI falls as the Span 80 concentration and hydration time rise [31]. Contour lines with labeled index values are included in both graphs to illustrate how the PDI changes with various variable combinations. Additional evidence for these conclusions comes from a perturbation plot that shows how sensitive the PDI is to variable variations. The perturbation plot (Figure 3d) supports the findings seen in the contour plots by showing that the concentration of Span 80 and the amount of phosphatidylcholine substantially impact the PDI.

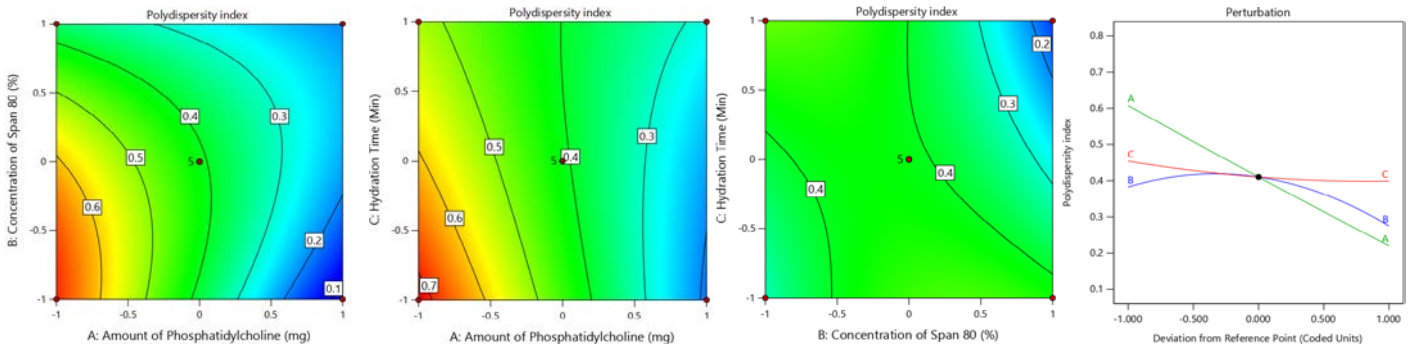

(a) (b) (c) (d)

Figure 3: Analyzing PDI variations with a) amount of phosphatidylcholine and concentration of Span 80, b) amount of phosphatidylcholine and hydration time, c) concentration of Span 80 and hydration time using contour plot, and d) perturbation plot

The X1 coefficient (-0.19) on vesicle size exhibits a negative effect, indicating an inverse relationship, as the amount of phosphatidylcholine increases. The association is evident in the perturbation plot and contour shown in Figure 3. The polynomial equation that resulted from regression analysis is as follows:

$$PDI = 0.41 - 0.19X_1 - 0.05X_2 - 0.03X_3 + 0.12X_1X_2 - 0.11X_2X_3 + 0.08X_1X_3 + 0.003X_1^2 - 0.08X_2^2 + 0.02X_3^2$$

A linear correlation plot comparing expected values on the y-axis with actual values on the x-axis is displayed in Figure 4a. There is a positive association between the expected and actual values, as evidenced by the data points forming an essentially linear trend. A box plot showing the distribution of a PDI is shown in Figure 4b. The horizontal line inside the box indicates the median value, and the box itself represents the IQR. Within 1.5 times the IQR, the whiskers reach the minimum and maximum values. The lack of outliers indicates that the data is comparatively centered around the median value [32].

Influence of independent variables on Zeta Potential (Y3)

The contour plots (Figure 5) show the relationship between the zeta potential (ZP) and various factors. Figure 5a shows how the zeta potential is affected by the concentration of Span 80 and the amount of phosphatidylcholine. It shows that when phosphatidylcholine and Span 80 concentrations are raised, the zeta potential decreases and moves from -5 mV to -15 mV. Higher concentrations of each component result in a considerable drop in zeta potential, indicating a strong dependence on them. This is often attributed to the adsorption of Span molecules onto the particle surface, efficiently neutralizing surface charges and reducing the zeta potential [33]. Similarly, Figure 5b, which investigates the correlation between phosphatidylcholine concentration and hydration time, displays a steady decline in zeta potential as both parameters rise from -7 mV to -11 mV. This suggests a more significant negative zeta potential from longer hydration durations and higher phosphatidylcholine concentrations.

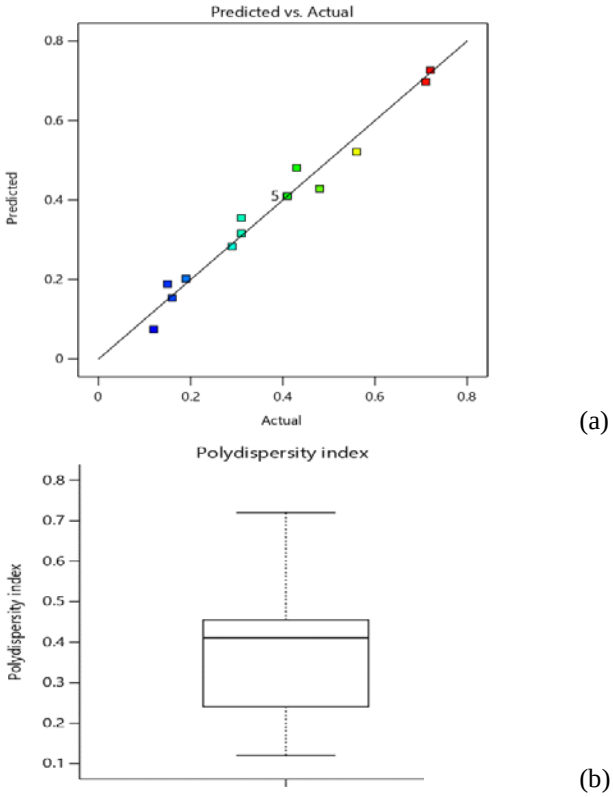

(a)

(b)

Figure 4: a) Linear correlation plot between actual and predicted values and b) Box plot for PDI of NBH transferosomes

Figure 5c illustrates how hydration time and Span 80 concentration affect zeta potential, showing a drop from -8 mV to -16 mV when these factors rise. This steep gradient suggests a high degree of reliance on both variables. The perturbation plot provides insight into the relative sensitivity of zeta potential to

variations in each element, demonstrating that Span 80 concentration has the most significant effect, followed by phosphatidylcholine quantity and hydration duration. The non-linear structure of the perturbation curve (Figure 5d) shows the complicated relationship between these parameters, especially at Span 80. These findings demonstrate that zeta potential is significantly affected by Span 80 concentration, phosphatidylcholine quantity, and hydration time, with each factor having a distinct effect on the total zeta potential. When developing transferosomes, zeta potential is a critical formulating property for transdermal medication administration. Because it suggests more vital repulsive forces between particles, which inhibit aggregation, a larger negative zeta potential usually indicates better stability of the vesicle suspension [34,35]. Stable transferosomes ensure more effective drug release profiles and encapsulation, which increases their efficacy in distributing medicinal compounds through the skin. The stability and efficacy of transferosomes in drug delivery applications might thus be strongly impacted by the noted differences in zeta potential with varying formulation parameters.

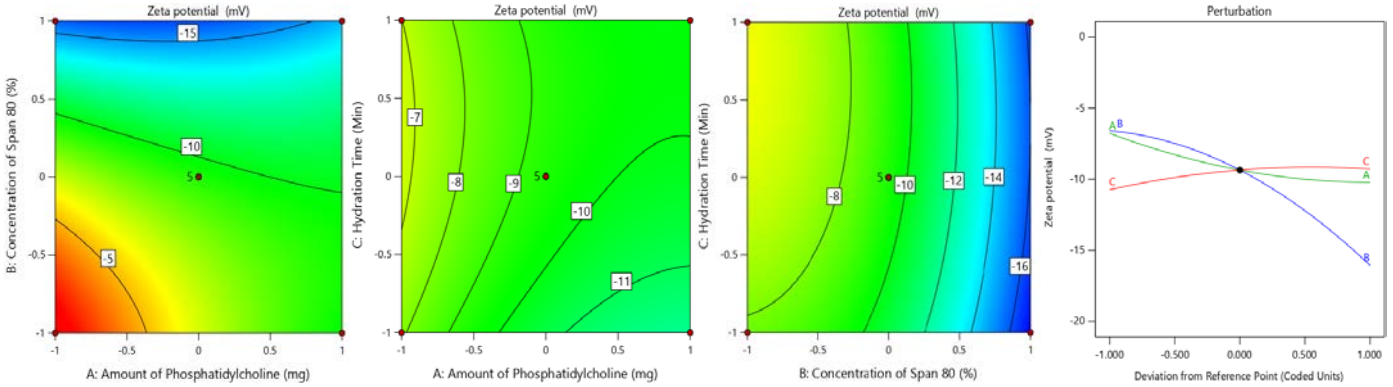

(a) (b) (c) (d)

Figure 5: Analyzing ZP variations with a) amount of phosphatidylcholine and concentration of Span 80, b) amount of phosphatidyl-choline and hydration time, c) concentration of Span 80 and hydration time using contour plot, and d) perturbation plot

The polynomial equation that resulted from regression analysis is as follows:

$ZP = -9.36 – 1.72X_1 – 4.73X_2 + 0.72X_3 + 2.38X_1X_2 – 0.27X_2X_3 + 0.28X_1X_3 + 0.87X_1^2 – 1.97X_2^2 – 0.66X_3^2$

The statistics provided insight into the distribution of zeta potential (ZP) for NBH transferosomes and the model's performance. The dark blue-to-red color gradient most likely depicts the range of values (Figure 6a). The distribution of ZP values is shown in Figure 6b, a box plot with a median of about -10 mV. The lack of outliers indicates a narrow distribution, and the interquartile range spans from -17 mV to -3 mV. The ZP values for NBH transferosomes are primarily negative, centered around -10 mV, and the model predictions are good overall [36].

Influence of independent variables on Entrapment Efficiency (Y4)

The amount of the entire drug (NBH) that is effectively encapsulated inside the transferosomes is denoted by EE. Because phosphatidylcholine is soluble in lipidic or aromatic hydrocarbon carriers but insoluble in polar solvents, it can efficiently generate vesicular structures resembling liposomes. The two-dimensional contour graphs for EE are shown in Figure 7, and the perturbation plot for EE is shown in Figure 7d. Higher phosphatidylcholine concentrations are associated with an increase in EE as confirmed by the perturbation plot and the corresponding two-dimensional contour plots. The perturbation plot also shows that EE increases with hydration time up to a certain threshold (Level 0); after this, additional increases in hydration time cause a slight rise in EE [37].

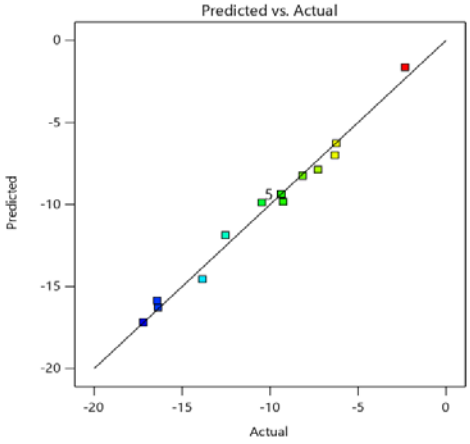

(a)

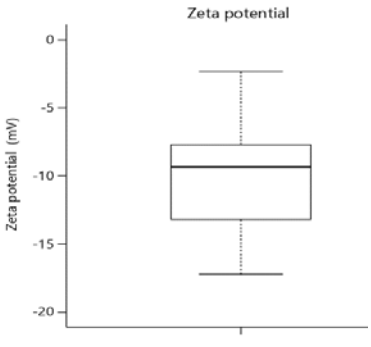

(b)

Figure 6: a) Linear correlation plot between actual and predicted values and b) Box plot for ZP of NBH transferosomes

Furthermore, it was noted that as Span 80 concentrations increased, the EE in transferosomes dropped. The quadratic equation 5 for EE supports these conclusions as, as Table 5 demonstrates, the coefficient for Span 80 concentration (b2) was negative (-3.59). This implies that increasing EE in transferosomes requires optimizing the amounts of phosphatidylcholine and span 80. It was also observed that the lipid composition and particular formulation parameters can impact the structural integrity and stability of the transferosomes. A greater concentration may cause the vesicular membrane to rupture, which would be consistent with the negative coefficient of Span 80 and result in a drop in EE [38]. Thus, to achieve the desired drug encapsulation efficiency, exact control over the formulation's ingredients and conditions is crucial. Subsequent research ought to investigate the interplay of distinct excipients and their influence on the general stability and efficacy of transferosome formulations. The polynomial equation that resulted from regression analysis is as follows:

$$EE = 50.29 + 7.54X_1 - 3.59X_2 + 4.46X_3 + 4.36X_1X_2 + 2.05X_2X_3 + 1.41X_1X_3 + 3.48X_1^2 + 2.64X_2^2 - 2.49X_3^2$$

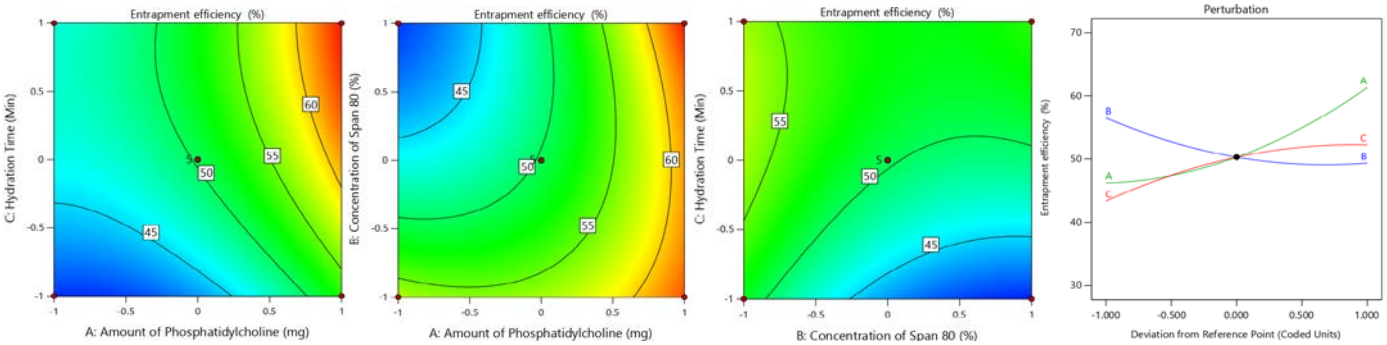

(a) (b) (c) (d)

Figure 7: Analyzing EE variations with a) amount of phosphatidylcholine and concentration of Span 80, b) amount of phosphatidyl-choline and hydration time, c) concentration of Span 80 and hydration time using contour plot, and d) perturbation plot

The given figure shows a linear correlation plot that shows the relationship between the EE of NBH transferosomes, as measured by actual and projected values. The line's evenly distributed points indicate that the model and the real data suit each other well. Figure 8a shows a strong linear relationship between the predicted and actual values, indicating that the model accurately predicts the NBH transferosomes' encapsulation efficiency.

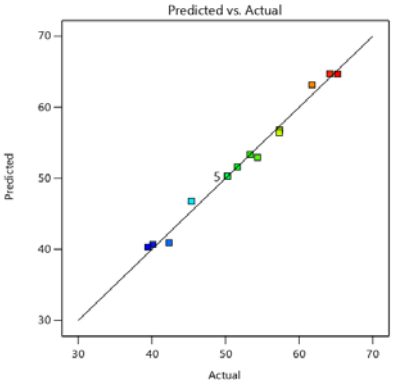

(a)

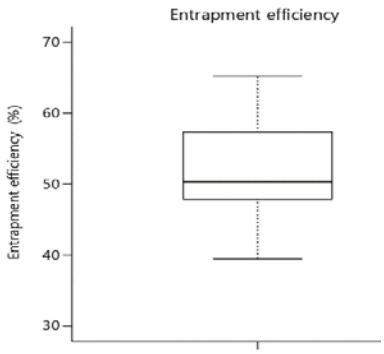

(b)

Figure 8: a) Linear correlation plot between actual and predicted values and b) Box plot for EE of NBH transferosomes

Optimization of Transferosomes

The best formulation had been achieved by selecting the Box-Behnken design due to its optimization significance. Achieving the smallest vesicle size, the maximum entrapment efficiency, the lowest polydispersity index, and confirming that the zeta potential value falls within the prescribed range allowed for

selecting the most effective formulation. The composition and expected response data are given in Table 5, and Figure 9 displays the corresponding overlay plot. To validate the design, the Design Expert software's suggested factor levels were used to create the optimal batch of transferosomes. Table 5 presents a minimal percent relative error comparison between the projected and experimental values, confirming the model's goodness of fit [39]. In transferosome formulation, the correlation between vesicle size and PDI is crucial for optimizing drug delivery. Smaller vesicles, typically 100-300 nm, are preferred for effective skin penetration, while a low PDI (< 0.3) ensures a uniform vesicle size distribution, leading to consistent drug release and formulation stability. The optimized transferosomes achieved a vesicle size of 265.24 nm and a PDI of 0.27. The vesicle size was ideal, and the PDI value indicates a fairly uniform size distribution, suggesting that the formulation is likely to be stable and capable of delivering the drug effectively. This balance between size and PDI in the optimized transferosomes enhances their potential for efficient and reliable transdermal drug delivery.

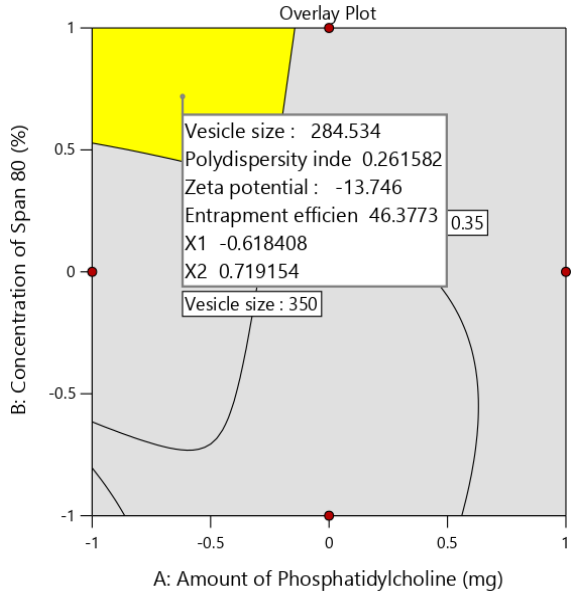

Figure 9: Overlay Plot for optimization of NBH transferosomes

Table 5. Performance evaluation of optimized NBH transferosomes

Response	*Predicted Value*	*Experimental Value [Mean ± SD (n=3)]*	*% Relative Error*
Vesicle size	284.53	265.24 ± 14.52	7.27%
Polydispersity index	0.26	0.27 ± 0.03	-3.70%
Zeta potential	-13.75	-12.96 ± 1.08	6.10%
Entrapment efficiency	46.37	50.03 ± 2.37	-7.32%

In Vitro Drug Diffusion Studies

In vitro drug diffusion of NBH was conducted and examined using a UV spectrophotometer at 282 nm. Throughout 24 hours, samples were taken out at prearranged intervals to calculate the percentage of drug permeation. The NBH exhibited an R^2 value of 0.9921 for the in vitro diffusion study (Figure 10), indicating that the formulation follows a zero-order kinetic pattern. Several kinetic models, such as Higuchi's model, Peppa's model, and the order of drug diffusion, were fitted to the data. An R^2 value of 0.937 was obtained from the Higuchi model (Figure 11a), which graphs cumulative drug release against the square root of time, suggesting a diffusion-controlled release mechanism [40]. This implies that the drug's diffusion across the carrier matrix is essentially responsible for controlling the drug's release from the transferosomes. Furthermore, Peppa's model (Figure 11b) yielded an R2 value of 0.993 and an n value of 0.978. It displays log(Q/Q∞) against log(t). The Peppa's model's high R^2 value denotes a very good match, and the n value near 1 point to a non-Fickian type release mechanism that is diffusion mediated [41]. These results emphasize the NBH formulation's features of controlled and predictable release. Furthermore, the robustness and dependability of the diffusion process are highlighted by the high R^2 values observed in several models. Figure 8 displays the in vitro drug diffusion plots depicting the drug release profile. The zero-order kinetic pattern shows a consistent medication release rate, which helps preserve stable therapeutic levels. Non-Fickian diffusion suggests a complex release mechanism that might incorporate diffusion and erosion processes. This thorough investigation confirms the formulation's effectiveness and offers insightful information for future optimization and development of comparable drug delivery methods. The NBH formulation's promise for clinical applications is reinforced by the stability and predictability of its release profile, which ensures efficient and long-lasting drug administration.

Physical Stability of the Transferosomes

The stability of the optimized NBH transferosomes has been evaluated by evaluating their physical appearance, drug content, and zeta potential under specified storage conditions over periods of 0, 3, and 6 months. These parameters were assessed

at room temperature for six months to ascertain the formulation's stability and dependability. However, none of the tested metrics showed significant changes, showing outstanding stability. Preserving physical characteristics is essential since any alterations in appearance may point to transferosome deterioration or aggregation (Table 6). The fact that the NBH transferosomes looked the same as before indicates that the vesicles were not precipitated or agglomerated. Its visual coherence is essential for both application efficiency and patient acceptance. According to the drug content analysis, the active component remained within the permitted range over the storage period. By ensuring that patients receive the appropriate dosage, this consistency upholds the formulation's therapeutic efficacy [42]. The fact that the drug content did not significantly degrade or disappear over time is evidence of the NBH's chemical stability within the transferosomal structure. A critical measure of a colloidal system's stability is its zeta potential. The zeta potential values of the NBH transferosomes remained stable, indicating that the vesicles retained their surface charge. This is crucial as it prevents aggregation and ensures consistent dispersion [43]. Additionally, stable zeta potential values suggest that the formulation will probably last longer on the shelf and continue to work for extended periods. Furthermore, the lack of significant differences in these parameters highlights the formulation's resistance to external elements, including humidity and temperature. This durability ensures that the NBH transferosomes can be utilized effectively in various situations without necessitating strict storage conditions, which is especially significant for storage and transit.

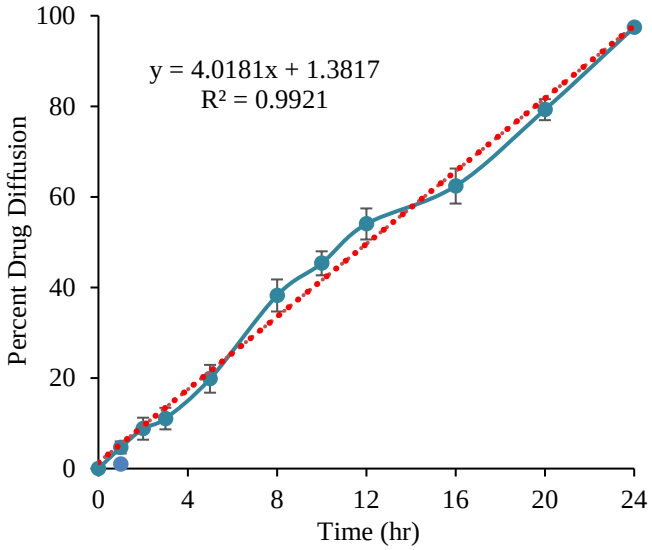

Figure 10: In vitro drug permeation of optimized NBH transferosomes

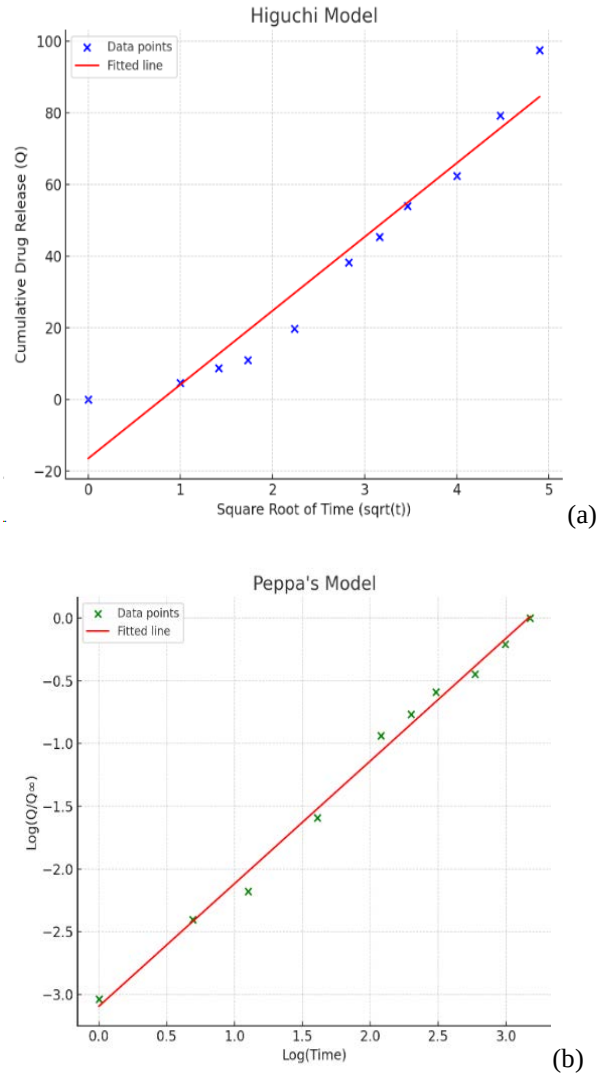

Figure 11 a) Higuchi model and b) Peppa's Model for kinetic study of NBH transferosomes

Table 6: Stability studies of optimized NBH transferosomes

Parameters	Storage Periods		
	Initial	3 months	6 months
Physical appearance	Clear	Clear	Clear
Zeta potential (mV)	-12.96 ± ± 1.08	-12.47 ± 1.14	-13.15 ± 0.74
NBH entrapment (%)	50.03 ± 2.37	49.57 ± 1.82	50.21 ± 1.29

* All results are the mean of three observations ± SD

CONCLUSIONS

Film hydration was utilized to load NBH and build the transferosomes properly. Critical responses, including vesicle size, zeta potential, polydispersity index (PDI), and entrapment efficiency (EE), were examined about the impacts of three independent variables: the amount of phosphatidylcholine, the

concentration of Span 80, and the length of time spent hydrated. This research utilized the response surface methodology based on the Box-Behnken design to find the ideal formulation. During 24 hours, the in vitro diffusion analysis showed zero-order drug release, indicating a steady and regulated release profile. Furthermore, stability studies demonstrated that the formulation did not significantly alter regarding zeta potential, drug content, or physical appearance over six months. The NBH transferosomes showed remarkable stability and a successful transdermal delivery mechanism. These highly deformable vesicles represent a substantial advancement in NBH delivery due to their robust architecture and constant performance, which ensures maintained therapeutic doses and increased patient compliance. This novel method increases NBH's bioavailability, and a viable platform for the transdermal distribution of other therapeutic agents is provided. Furthermore, the thorough assessment and optimization procedure highlight the NBH transferosomes' potential for scalability and commercial feasibility. Subsequent investigations may examine additional enhancements in formulation and the feasibility of conducting clinical trials to validate these results in a more extensive patient cohort. The accomplishments of this study provide a strong foundation for the further advancement and use of transferosomal technology in drug administration systems.

FINANCIAL ASSISTANCE
NIL

CONFLICT OF INTEREST
The authors declare no conflict of interest.

AUTHOR CONTRIBUTION
P V Shelke conceptualized the research idea, provided oversight for the project, and supervised the experimental design. Played a crucial role in critically analyzing and approving the final manuscript. Punit R. Rachh led the formulation and optimization of Nebivolol Hydrochloride-loaded transferosomes. Conducted the majority of the experimental work and contributed to data analysis and interpretation. Someshwar Mankar assisted in applying the Box-Behnken experimental design for optimization and performed statistical analysis. Involved in the drafting and reviewing of the results section. Saurin Amin contributed to the literature review and supported the optimization process by conducting stability studies. Played a role in manuscript writing, especially in the introduction and discussion sections. Deepak Jain was involved in data interpretation, provided feedback on statistical methodologies, and reviewed the manuscript critically for important intellectual content. Assisted with the revision process and ensured accuracy in reporting the results.

REFERENCES
[1] Alkilani AZ, Nasereddin J, Hamed R, Nimrawi S, Hussein G, Abo-Zour H, et al. Beneath the skin: a review of current trends and future prospects of transdermal drug delivery systems. *Pharmaceutics*, **14(6)**, 1152 (2022).

[2] Ahad A, Al-Mohizea AM, Al-Jenoobi FI, Aqil M. Transdermal delivery of angiotensin II receptor blockers (ARBs), angiotensin-converting enzyme inhibitors (ACEIs) and others for management of hypertension. *Drug Delivery*, **23(2)**, 579-90 (2016).

[3] Tanwar H, Sachdeva R. Transdermal drug delivery system: A review. *International Journal of Pharmaceutical Sciences and Research*, **7(6)**, 2274 (2016).

[4] Sabbagh F, Kim BS. Recent advances in polymeric transdermal drug delivery systems. *Journal of Controlled Release*, **341**, 132-46 (2022).

[5] Hedaya MA. Routes of Drug Administration. In: Dash AK, Singh S, editors. *Pharmaceutics*. Academic Press, 537-554 (2024).

[6] Hemrajani C, Negi P, Parashar A, Gupta G, Jha NK, Singh SK, et al. Overcoming drug delivery barriers and challenges in topical therapy of atopic dermatitis: A nanotechnological perspective. *Biomedicine & Pharmacotherapy*, **147**, 112633 (2022).

[7] Üstündağ-Okur N, Yurdasiper A, Gündoğdu E, Homan Gökçe E. Modification of solid lipid nanoparticles loaded with nebivolol hydrochloride for improvement of oral bioavailability in treatment of hypertension: Polyethylene glycol versus chitosan oligosaccharide lactate. *Journal of Microencapsulation*, **33(1)**, 30-42 (2016).

[8] Shah A, Gandhi D, Srivastava S, Shah KJ, Mansukhani R. Heart failure: A class review of pharmacotherapy. *Pharmacy and Therapeutics*, **42(7)**, 464-472 (2017).

[9] Farhoumand LS, Liu H, Tsimpaki T, Hendgen-Cotta UB, Rassaf T, Bechrakis NE, et al. Blockade of ß-adrenergic receptors by nebivolol enables tumor control potential for uveal melanoma in 3D tumor spheroids and 2D cultures. *International Journal of Molecular Sciences*, **24(6)**, 5894 (2023).

[10] Matharoo N, Mohd H, Michniak-Kohn B. Transferosomes as a transdermal drug delivery system: Dermal kinetics and

recent developments. *Wiley Interdisciplinary Reviews: Nanomedicine and Nanobiotechnology*, **16(1)**, e1918 (2024).

[11] Garala KC, Patel JM, Dhingani AP, Dharamsi AT. Preparation and evaluation of agglomerated crystals by crystallo-co-agglomeration: an integrated approach of principal component analysis and Box–Behnken experimental design. *International Journal of Pharmaceutics*, **452(1-2)**, 135-56 (2013).

[12] Fernández-García R, Lalatsa A, Statts L, Bolás-Fernández F, Ballesteros MP, Serrano DR. Transferosomes as nanocarriers for drugs across the skin: Quality by design from lab to industrial scale. *International Journal of Pharmaceutics*, **573**, 118817 (2020).

[13] Abdallah MH, Abu Lila AS, Shawky SM, Almansour K, Alshammari F, Khafagy E-S, et al. Experimental design and optimization of nano-transfersomal gel to enhance the hypoglycemic activity of silymarin. *Polymers*, **14(3)**, 508 (2022).

[14] Lei W, Yu C, Lin H, Zhou X. Development of tacrolimus-loaded transfersomes for deeper skin penetration enhancement and therapeutic effect improvement in vivo. *Asian Journal of Pharmaceutical Sciences*, **8(6)**, 336-345 (2013).

[15] Raval MK, Garala KC, Patel JM, Parikh RK, Sheth NR. Functionality improvement of chlorzoxazone by crystallo-co-agglomeration using multivariate analysis approach. *Particulate Science and Technology*, **39(6)**, 689-711 (2021).

[16] Kharwade R, Ali N, Gangane P, Pawar K, More S, Iqbal M, et al. DOE-assisted formulation, optimization, and characterization of tioconazole-loaded transferosomal hydrogel for the effective treatment of atopic dermatitis: in vitro and in vivo evaluation. *Gels*, **9(4)**, 303 (2023).

[17] Rarokar NR, Saoji SD, Deole NV, Gaikwad M, Pandey A, Kamaraj C, et al. Preparation and formula optimization of cephalexin-loaded transferosomal gel by QbD to enhance the transdermal delivery: in vitro, ex vivo, and in vivo study. *Journal of Drug Delivery Science and Technology*, **89(1)**, 104968 (2023).

[18] Zaky A. Comparative study of terbinafine hydrochloride transfersome, menthosome, and ethosome nanovesicle formulations via skin permeation and antifungal efficacy. *Al-Azhar Journal of Pharmaceutical Sciences*, **54(1)**, 18-36 (2016).

[19] Tamilarasan N, Yasmin BM, Anitha P, Umme H, Cheng WH, Mohan S, et al. Box–Behnken design: optimization of proanthocyanidin-loaded transferosomes as an effective therapeutic approach for osteoarthritis. *Nanomaterials*, **12(17)**, 2954 (2022).

[20] Saha R, Patkar S, Maniar D, Pillai MM, Tayalia P. A bilayered skin substitute developed using an eggshell membrane crosslinked gelatin–chitosan cryogel. *Biomaterials Science*, **9(23)**, 7921-33 (2021).

[21] Garala KC, Shah PH. Influence of crosslinking agent on the release of drug from the matrix transdermal patches of HPMC/Eudragit RL 100 polymer blends. *Journal of Macromolecular Science®, Part A: Pure and Applied Chemistry*, **47**(3), 273-81 (2010).

[22] Yameen SH, Shahidulla S. Formulation and evaluation of lamivudine transferosomal gel. *Journal of Drug Delivery and Therapeutics*, **12(4-S)**, 163-70 (2022).

[23] Basu B, Garala KK, Patel R, Dutta A, Ash D, Prajapati B, et al. Advanced targeted drug delivery of bioactive nanomaterials in the management of cancer. *Current Medicinal Chemistry*, **31(1)** (2024).

[24] Dhingani A, Patel J, Garala K, Raval M, Dharamsi A. Quality by design approach for development of W/O type microemulsion-based transdermal systems for atenolol. *Journal of Dispersion Science and Technology*, **35**(5), 619-40 (2014).

[25] Garala KC, Patel JM, Dhingani AP, Dharamsi AT. Quality by design (QbD) approach for developing agglomerates containing racecadotril and loperamide hydrochloride by crystallo-co-agglomeration. *Powder Technology*, **247**, 128-46 (2013).

[26] Bnyan R, Khan I, Ehtezazi T, Saleem I, Gordon S, O'Neill F, et al. Surfactant effects on lipid-based vesicles properties. *Journal of Pharmaceutical Sciences*, **107(5)**, 1237-46 (2018).

[27] Guo H-Y, Sun H-Y, Deng G, Xu J, Wu F-G, Yu Z-W. Fabrication of asymmetric phosphatidylserine-containing lipid vesicles: a study on the effects of size, temperature, and lipid composition. *Langmuir*, **36(42)**, 12684-91 (2020).

[28] Ismail A, Teiama M, Magdy B, Sakran W. Development of a novel bilosomal system for improved oral bioavailability of sertraline hydrochloride: Formulation design, in vitro characterization, and ex vivo and in vivo studies. *AAPS PharmSciTech*, **23(6)**, 188 (2022).

[29] Opatha SAT, Titapiwatanakun V, Boonpisutiinant K, Chutoprapat R. Preparation, characterization and permeation study of topical gel loaded with transfersomes containing asiatic acid. *Molecules*, **27(15)**, 4865 (2022).

[30] Fatima A, Quraishi N, Babu MS. Formulation and in-vitro evaluation of gabapentin-loaded transferosomal gel. *Journal of Drug Delivery and Therapeutics*, **13(12)**, 60-70 (2023).

[31] Cheng Z, Kandekar U, Ma X, Bhabad V, Pandit A, Liu L, et al. Optimizing fluconazole-embedded transfersomal gel for enhanced antifungal activity and compatibility studies. *Frontiers in Pharmacology*, **15**, 1353791 (2024).

[32] Ahmed IF, Alheyf M, Yamany MS. PlanetiQ Radio Occultation: preliminary comparative analysis of neutral profiles vs. COSMIC and NWP models. *Applied Sciences*, **14(10)**, 4179 (2024).

[33] Ma X, Li M, Xu X, Sun C. On the role of surface charge and surface tension tuned by surfactant in stabilizing bulk nanobubbles. *Applied Surface Science*, **608**, 155232 (2023).

[34] Pan L, Meng H, Li J, Liu Z, Zhang D, Liu Z, et al. Enhancement of astaxanthin bioaccessibility by encapsulation in liposomes: an in vitro study. *Molecules*, **29(8)**, 1687 (2024).

[35] Buddhadev SS, K CG, S S, Rahamathulla M, Ahmed MM, Farhana SA, et al. Quality by design aided self-nano emulsifying drug delivery systems development for the oral delivery of benidipine: improvement of biopharmaceutical performance. *Drug Delivery*, **31(1)**, 2288801 (2024).

[36] Guzik P, Więckowska B. Data distribution analysis–a preliminary approach to quantitative data in biomedical research. *Journal of Medical Science*, **92(2)**, 869 (2023).

[37] Barekat S, Nasirpour A, Keramat J, Dinari M, Claeys M, Sedaghat Doost A, et al. Formulation, characterization, and physical stability of encapsulated walnut green husk (Juglans regia L.) extract in phosphatidylcholine liposomes. *Journal of Dispersion Science and Technology*, **45(11)**, 2180–2193 (2023).

[38] Yasser M, El Naggar EE, Elfar N, Teaima MH, El-Nabarawi MA, Elhabal SF. Formulation, optimization and evaluation of ocular gel containing nebivolol HCl-loaded ultradeformable spanlastics nanovesicles: in vitro and in vivo studies. *International Journal of Pharmaceutics:* **10(7),** 100-228 (2024).

[39] Garala K, Joshi P, Shah M, Ramkishan A, Patel J. Formulation and evaluation of periodontal in situ gel. *International Journal of Pharmaceutical Investigation*, **3(1)**, 29 (2013).

[40] Unagolla JM, Jayasuriya AC. Drug transport mechanisms and in vitro release kinetics of vancomycin encapsulated chitosan-alginate polyelectrolyte microparticles as a controlled drug delivery system. *European Journal of Pharmaceutical Sciences*, **114**, 199-209 (2018).

[41] Bayer IS. Controlled drug release from nanoengineered polysaccharides. *Pharmaceutics*, **15(5)**, 1364 (2023).

[42] Kapoor DU, Garg R, Gaur M, Patel MB, Minglani VV, Prajapati BG, et al. Pediatric drug delivery challenges: enhancing compliance through age-appropriate formulations and safety measures. *Journal of Drug Delivery Science and Technology*, **105720** (2024).

[43] Németh Z, Csóka I, Semnani Jazani R, Sipos B, Haspel H, Kozma G, et al. Quality by design-driven zeta potential optimisation study of liposomes with charge imparting membrane additives. *Pharmaceutics*, **14(9)**, 1798 (2022).